[3] T. T. Dabrah, H. J. Harwood, Jr., L. H. Huang, N. D. Jankovich, T. Kaneko, J.-C. Li, S. Lindsey, P. M. Moshier, T. A. Subashi, M. Therrien, P. C. Watts, *J. Antibiot*. **1997**, 50, 1.
[4] The ratio varied between 8:1 to 10:1 in favor of **6**. The Heck closure of the unprotected **6** was also accomplished, but in much lower yield and with poor reproducibility.
[5] a) D. B. Dess, J. C. Martin, *J. Org. Chem*. **1983**, 48, 4155; b) R. E. Ireland, L. Liu, *J. Org. Chem*. **1993**, 58, 2899.
[6] Compound **12** was recovered after exposure to the conditions of the Wittig or Wadsworth–Emmons–Horner condensation. Similarly, it was unreactive toward the corresponding antimony ylide ($SbBu_3$, $N_2CH_2CO_2CH_3$, CuI (cat.), PhH, 50 °C). Addition of lithium ethoxyacetylide provided only a 21% yield of a tertiary alcohol (with 43% starting material recovered). The formation of the corresponding $\alpha,\beta$-unsaturated ester from this product was not successful. A Peterson-type reaction with ethyl lithiotrimethylsilylacetate afforded only a 28% yield of the $\alpha,\beta$-unsaturated ester (with 34% starting material recovered). By contrast, Reformatsky reaction provided almost complete transformation to a $\beta$-hydroxy ester. However, dehydration of this compound has thus far not been achieved. A modified Reformatsky reaction (with methyl dichloroacetate and Zn in the presence of diethylaluminum chloride: K. Takai, Y. Hotta, K. Oshima, H. Nozaki, *Bull. Chem. Soc. Jpn*. **1980**, *53*, 1698) produced the $\alpha,\beta$-unsaturated ester in 73% yield. Early attempts to deliver a one-carbon fragment to the enoate have not been productive. Given our success in spirobutanone formation, these studies have not yet been pursued in detail.
[7] B. M. Trost, M. J. Bogdanowicz, *J. Am. Chem. Soc.***1973**, 95, 5311.
[8] B. M. Trost, M. J. Bogdanowicz, *J. Am. Chem. Soc.***1973**, 95, 5321.
[9] B. M. Trost, J. H. Rigby, *J. Org. Chem*. **1976**, 41, 3217.
[10] At the present time we cannot be certain whether lactone formation occurs upon acidification of the product obtained upon opening of the four-membered ring (*seco*-cleavage product) or by the more interesting possibility wherein the C1 hydroxyl participates as the nucleophile in the cleavage step following bis-sulfenylation.
[11] M. R. Kernan, D. J. Faulkner, *J. Org. Chem*. **1988**, 53, 2773.
[12] S. R. Magnuson, L. Sepp-Lorenzino, N. Rosen, S. J. Danishefsky, *J. Am. Chem. Soc.***1998**, 120, 1615.
[13] Selected physical properties for **25**: $^1$H NMR (400 MHz, $CDCl_3$): $\delta =$ 7.22 (d, $J = 8.6$ Hz, 2H), 6.84 (d, $J = 6.8$, 2.1 Hz, 2H), 5.34 (t, $J =$ 5.6 Hz, 1H), 5.12 (d, $J = 5.6$ Hz, 1H), 4.39 (s, 2H), 3.93 (dt, $J =$ 11.4 Hz, 1H), 3.77 (s, 3H), 3.58 (t, $J = 5.7$ Hz, 1H), 3.40 (t, $J =$ 6.5 Hz, 2H), 2.69 (dd, $J = 5.6$, 0.9 Hz, 1H), 2.53 (m, 3H), 2.31 (dd, $J = 10.2$ Hz, 1H), 2.02 (s, 3H), 1.58 (m, 4H), 1.28 (m, 6H), 0.85 (s, 9H), 0.039 (s, 3H), 0.007 (s, 3H); FT-IR (neat): 1771, 1698, 1558, 1508, 1248, 1091 $cm^{-1}$; LR-MS calcd for $C_{34}H_{48}O_8SiNa$: 635.3, found: 635.3 [$M$+Na].
[14] The construction of the C5–C6 bridgehead double bond has been accomplished recently: D. Meng, Columbia University, unpublished results.

# Direct Observation of Fluid Mass Transfer Resistance in Porous Media by NMR Spectroscopy**

Ulrich Tallarek, Dagmar van Dusschoten, Henk Van As, Georges Guiochon, and Ernst Bayer*

*In memory of John Calvin Giddings*

The transport of solutes by dispersion, a combination of convection and hindered diffusion, through heterogeneous porous media is of fundamental importance in many areas such as liquid chromatography,[1, 2] catalysis,[3] the migration of pollutants in groundwater,[4] and petroleum recovery.[5] Most porous media exhibit bi- or multimodal pore-size distributions, which can result, for example, from the intraparticle and interparticle pores in beds of porous particles, as are used in chromatographic columns.[1, 6] Although the kinetics of mass transfer between the fluid percolating through the system and the stagnant fluid in the diffusional pores is known to be the rate-limiting step in numerous dynamic processes (e.g., the efficiency of chromatographic columns[2] or the amount of oil that can be economically recovered from a reservoir), no direct, quantitative measurement of these kinetics has been provided so far. Here we show how the pulsed field gradient (PFG) NMR method[7] allows the determination of these kinetics. A single series of measurements permits the identification of the stagnant fluid fraction, of the fractional volume exchanged as a function of time, and of the porosity and tortuosity of the porous medium.

Figure 1 illustrates the structure of a bed of porous particles as used in column chromatography or in heterogeneous catalysis. Permeable rocks have a more complex porous structure, with a multimodal pore-size distribution and interconnection of the pores.[8] However, water and oil bypass regions containing networks of finer pores by flowing through cracks. The fluid pools inside zones with fine pores are only accessible by diffusion. In chromatography, axial dispersion of a band arises from axial diffusion along the streamlines, eddy diffusion (resulting from the anastomosis of the porous space and the differences in the average velocity along streamlines), and the kinetics of mass transfer into and out of the particles.[2]

[*] Prof. Dr. E. Bayer, Dr. U. Tallarek
Institut für Organische Chemie der Universität
Auf der Morgenstelle 18, D-72076 Tübingen (Germany)
Fax: (+49) 7071-29-5034
E-mail: ernst.bayer@uni-tuebingen.de
Dr. D. van Dusschoten, Dr. H. Van As
Department of Molecular Physics & Wageningen NMR Centre
Wageningen Agricultural University
Dreijenlaan 3, NL-6703 HA Wageningen (The Netherlands)
Prof. Dr. G. Guiochon
Department of Chemistry, University of Tennessee at Knoxville
Knoxville, TN 37996-1600 (USA)
and
Chemical and Analytical Sciences Division
Oak Ridge National Laboratory
Oak Ridge, TN 37831 (USA)

[**] This work was supported in part by a Human Capital and Mobility Grant of the European Union, by a grant of the U.S. Department of Energy, and by the Deutsche Forschungsgemeinschaft.

  1433-7851/98/3713-1882 $ 17.50+.50/0 

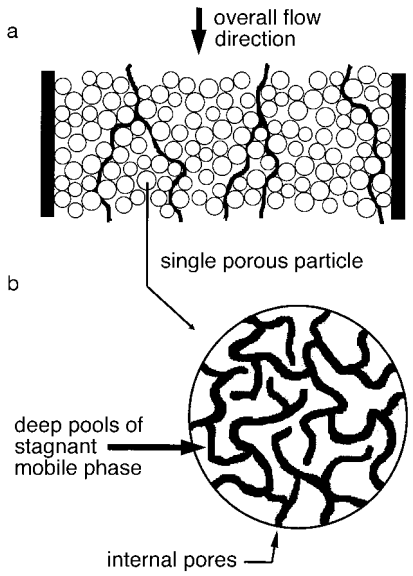


Figure 1. Schematic representation of the structure of a bed of porous particles and distribution of a fluid phase. a) Tortuous streamlines followed by the fluid percolating through the coarse pores between and around particles. b) Stagnant fluid in the fine pores of the particles. Exchange with the interparticular fluid stream occurs by diffusion only.

Since these phenomena proceed on different dynamic time scales, their contributions to band dispersion can be determined independently and quantitatively by the PFG-NMR method. In these studies a single pure liquid phase continuously flows through the bed, which avoids extracolumn band broadening and problems with NMR detection limits that could arise if a tracer molecule were introduced.[9]

The PFG-NMR method utilizes the motion-encoding capability of a linear magnetic field gradient superimposed for a short time on the main, static magnetic field.[7] A second, identical gradient pulse, separated from the first pulse by an adjustable observation time $\Delta$, exactly compensates the position-dependent phase shift induced by the first gradient if the molecule carrying the nuclear spin ($^1H_2O$) has remained static with respect to the direction of this gradient. Thus, the distribution of the residual net phase shifts results directly from the dynamics of the fluid molecules over this time $\Delta$. In an ideal PFG-NMR experiment,[10] the normalized signal amplitude $E(\boldsymbol{q},\Delta)$ is given by Equation (1).

$$E(\boldsymbol{q},\Delta) = \int \bar{P}(\boldsymbol{R},\Delta)\exp(i2\pi\boldsymbol{q}\cdot\boldsymbol{R})\mathrm{d}\boldsymbol{R} \qquad (1)$$

In this equation, the gradient integral defines a wave-vector,[11] $\boldsymbol{q} = (2\pi)^{-1}\gamma\delta\boldsymbol{g}$, which is the space reciprocal of the dynamic displacement $\mathbf{R}$; $\boldsymbol{g}$ is the amplitude and direction of the pulsed field gradient, $\delta$ its duration ($\delta \ll \Delta$), and $\gamma$ the magnetogyric ratio of the observed nucleus (here $^1H$). The quantity $\bar{P}(\boldsymbol{R},\Delta)$, which exhibits a direct Fourier relationship with the measured NMR signal, is the displacement probability distribution of the fluid molecules and is known as the averaged propagator.[12] Hence, the distribution of net (i.e., dynamic) displacements of the fluid molecules can be derived from the measured signal by Fourier transformation of $E(\boldsymbol{q},\Delta)$ with respect to $\boldsymbol{q}$. Adjusting the observation time and the flow velocity of the fluid phase allows a detailed investigation of the mass transfer kinetics between the stagnant and the mobile volume fractions of the fluid.

For classical convective fluid dispersion in a packed bed of nonporous particles, the distribution of migration distances $\boldsymbol{R}$ is Gaussian[13] and the averaged propagator $\bar{P}(\boldsymbol{R},\Delta)$ along the net flow direction is given by Equation (2).

$$\bar{P}(\boldsymbol{R},\Delta) = \frac{1}{\sqrt{2\pi\sigma^2}}\exp\left[\frac{-(\boldsymbol{R}-\bar{\boldsymbol{u}}\Delta)^2}{2\sigma^2}\right] \qquad (2)$$

Here, $\bar{\boldsymbol{u}}$ is the cross-sectional average of the fluid phase linear velocity, and $\sigma^2 = 2D_{ap}\Delta$ the distribution variance. Thus, for a bed of nonporous particles, the apparent dispersion coefficient of the fluid in the gradient direction $D_{ap}$ and the velocity of the mobile phase $\bar{\boldsymbol{u}}$ can be derived from the standard deviation $\sigma$ and the center position of the maximum ($\bar{\boldsymbol{u}}\Delta$) of this Gaussian distribution, respectively.

With porous particles, by contrast, the spectrum of fluid displacements contains two Gaussian distributions if the exchange between the inter- and intraparticle fluids is incomplete (Figures 2 and 3). The first Gaussian distribution-corresponds to molecules that migrate with the fluid stream which percolates through the bed. The second Gaussian distribution is centered at $\boldsymbol{R} = 0$ and corresponds to diffusion of the molecules of stagnant fluid in the pores of the particles (Figure 1). The ratio of the areas under these two curves provides an estimate of the fraction of molecules in the stagnant fluid that did not undergo exchange with molecules of the stream during the time interval $\Delta$. This fraction decreases with increasing observation (exchange) time. For a given observation time, this fraction is higher for 50-μm particles than for 15-μm particles (Figures 2 and 3). Figure 2

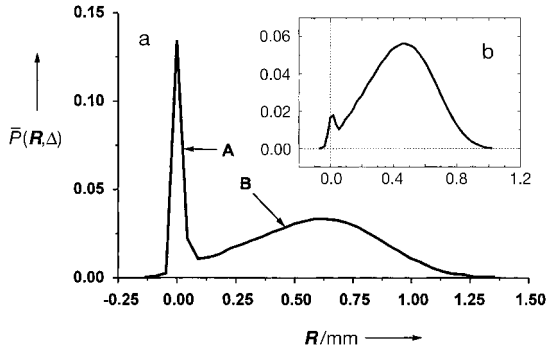


Figure 2. Probability distribution of the displacement of water molecules in two columns packed with spherical, totally porous, $C_{18}$-functionalized silica particles (YMC Europe, Schermbeck, Germany). Intraparticle pore-size distribution: $13 \pm 1.5$ nm; flow rate $F_v = 8.8\,\mathrm{mL\,min^{-1}}$; observation time $\Delta = 30$ ms ($\delta = 4.0$ ms); fluid phase: pure, degassed water. The columns ($4.4 \times 150$ mm) were slurry-packed according to conventional practice.[1] PFG-NMR measurements were performed with a 0.5-T NMR spectrometer consisting of an SMIS console (Surrey Medical Imaging Systems, Guildford, UK), an iron-core magnet (Bruker, Karlsruhe, Germany), and an actively shielded gradient and RF probe (Doty Scientific, Columbia, OH, USA). a) Average particle diameter $d_p = 50$ μm. The first Gaussian curve (A, stagnant fluid fraction, 21%) is centered at zero net displacement, and the second Gaussian curve (B, flowing fluid fraction, 79%) at a dynamic displacement of $\bar{\boldsymbol{u}}\Delta = 0.638$ mm with a standard deviation of $\sigma_1 = 0.365$ mm. b) $d_p = 15$ μm. The stagnant fluid fraction at the same observation time is only 2.5%. The maximum of the Gaussian curve that describes the flowing fluid is located at $\bar{\boldsymbol{u}}\Delta = 0.463$ mm ($\sigma_1 = 0.215$ mm).

  1433-7851/98/3713-1883 $ 17.50+.50/0 

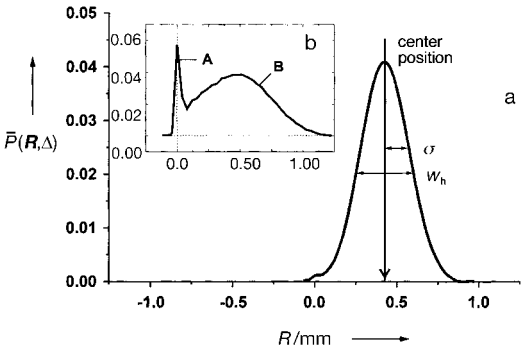


Figure 3. As in Figure 2, but with $F_v = 2.2\ \mathrm{mL\,min^{-1}}$ and $\Delta = 120$ ms. a) $d_p = 15\ \mu$m. The stagnant fluid fraction is almost completely exchanged (residual fraction $< 1\,\%$). The center of the Gaussian distribution is at $\bar{\boldsymbol{u}}\Delta = 0.445$ mm ($\sigma_1 = 0.145$ mm). b) $d_p = 50\ \mu$m. Stagnant fluid fraction: 8.5 % (A); flowing fluid fraction: 91.5 % (B). The first Gaussian distribution is centered at the origin, and the second at a net displacement $\bar{\boldsymbol{u}}\Delta = 0.482$ mm and has a standard deviation of $\sigma_1 = 0.276$ mm.

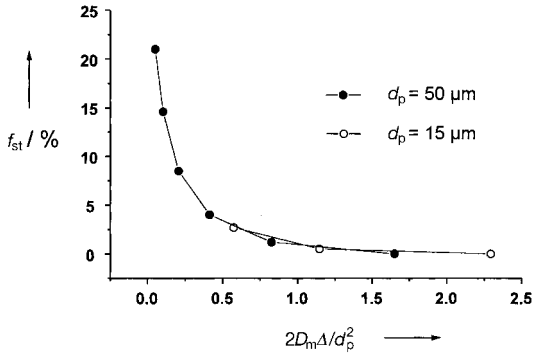


Figure 4. Plot of the stagnant fluid fraction $f_{st}$ that remained unexchanged after time $\Delta$ versus the Fick number ($2D_m\Delta/d_p^2$). The observation time was increased stepwise from 30 to 960 ms for the 50-µm particles, and from 30 to 120 ms for the 15-µm particles.

shows that at the shortest observation time ($\Delta = 30$ ms), 21 % of the fluid is stagnant in the column with the larger particles, and only 2.5 % in the column with the smaller particles.

After 120 ms practically all the fluid contained in the 15-µm particles was exchanged (Figure 3 a), while 8.5 % of the stagnant fluid remained unexchanged in the 50-µm particles (Figure 3 b). The widths at half height of the two Gaussian distributions can be used to determine the apparent dispersion coefficients of the fluid in the respective pore spaces relative to their porosities and tortuosities. From the averaged propagator distributions shown in Figure 3 b, an apparent axial dispersion coefficient of $D_{ap,1} = \sigma_1^2/2\Delta = 3.18 \times 10^{-3}\ \mathrm{cm^2\,s^{-1}}$ in the extraparticle space and a diffusion coefficient of $D_{ap,2} = 1.05 \times 10^{-5}\ \mathrm{cm^2\,s^{-1}}$ in the intraparticle space were calculated. The molecular diffusivity of pure water (unhindered diffusion) was determined by PFG-NMR to be $D_m = 2.15 \times 10^{-5}\ \mathrm{cm^2\,s^{-1}}$ at 23 °C. Therefore, the tortuosity factor of the intraparticle pore network is $D_{ap,2}/D_m = 0.51$, a reasonable value for a complicated pore network.[3] This geometrical parameter is an important characteristic of the pore interconnectivity in porous media. So far, its direct determination was extremely difficult and inaccurate.

When exchange between the two fluid fractions is complete, a single Gaussian distribution is observed. It includes the whole contribution to axial dispersion of the resistance to mass transfer between stagnant and mobile fluid phases (Figure 3). Then, the column or total bed porosity $\varepsilon_T$ is easily derived from the average velocity $|\bar{\boldsymbol{u}}\Delta| = 4F_v/\varepsilon_T\pi d_c^2$ ($d_c$ = column diameter, $F_v$ = volumetric flow rate), which itself is derived from the position of the maximum of the Gaussian curve (at $\bar{\boldsymbol{u}}\Delta$). Values of 0.67 and 0.65 were obtained for the 50- and 15-µm particles, respectively, in excellent agreement with data obtained from independent chromatographic determinations.[14]

In Figure 4 the stagnant fluid fraction $f_{st}$ is plotted versus the Fick number ($2D_m\Delta/d_p^2$). The use of the Fick number normalizes the data with respect to the particle diameter and provides an estimate of the time required for equilibration of the compositions of the stagnant fluid and of the fluid percolating through the bed. The coincidence between the data obtained for the two materials studied was expected since they have the same origin. This result demonstrates the redundant nature of fluid mass transfer resistance in similar pore networks and provides a useful basis for a comparison between different pore spaces.

The use of columns made of poly(aryl ether ether ketone) (PEEK) was critical for obtaining meaningful results. This polymer has high tensile strength and thus permits the packing and operation of columns under conditions realistic for chromatographic applications (up to 350 bar) and the recording of NMR data which are relevant to problems encountered in the study of the properties of consolidated beds of particles.[15] The implementation is straightforward and is an improvement over the loose, centrifuged arrays of particles that are obtained in conventional NMR tubes and through which solvent percolation is not possible.[16]

The great potential and broad application of these PFG-NMR studies lies in the ability to determine a variety of important parameters that characterize the fluid dynamics in porous media in a single measurement, performed in less than 15 min. Such mass transfer studies can be performed on any type of porous material in which a fluid is exchanged within and between a microporous and macroporous pore networks. Such situations are found in groundwater transport, in the transport of water between soil and plants, in fermentors, and in the various packed beds used in chemical engineering.

Received: February 26, 1998 [Z 11521 IE]
German version: *Angew. Chem.* **1998**, *110*, 1983 – 1986

**Keywords:** analytical methods · liquid chromatography · mass transfer · NMR spectroscopy · porous materials

[1] C. F. Poole, S. K. Poole, *Chromatography Today*, 2nd ed., Elsevier, Amsterdam, **1993**.
[2] G. Guiochon, S. Golshan-Shirazi, A. M. Katti, *Fundamentals of Preparative and Nonlinear Chromatography*, Academic Press, Boston, MA, **1994**.
[3] C. N. Satterfield, *Mass Transfer in Heterogeneous Catalysis*, MIT Press, Cambridge, MA, **1970**.
[4] J. Bear, *Hydraulics of Groundwater*, McGraw-Hill, New York, NY, **1979**.
[5] L. Lake, *Enhanced Oil Recovery*, Prentice-Hall, Clifton, NJ, **1992**.
[6] U. D. Neue, *HPLC Columns*, Wiley, New York, NY, **1997**.

  1433-7851/98/3713-1884 $ 17.50+.50/0 

[7] P. T. Callaghan, *Principles of Nuclear Magnetic Resonance Microscopy*, Clarendon Press, Oxford, **1993**.
[8] M. Sahimi, *Flow and Transport in Porous Media and Fractured Rocks*, VCH, Weinheim, **1995**.
[9] U. Tallarek, E. Bayer, G. Guiochon, *J. Am. Chem. Soc.* **1998**, *120*, 1494 – 1505.
[10] E. O. Stejskal, J. E. Tanner, *J. Chem. Phys.* **1965**, *42*, 288 – 292.
[11] P. T. Callaghan, A. Coy, D. MacGowan, K. J. Packer, F. O. Zelaya, *Nature* **1991**, *351*, 467 – 469.
[12] J. Kärger, W. Heink, *J. Magn. Reson.* **1983**, *51*, 1 – 7.
[13] D. J. Gunn, *Trans. Instn. Chem. Eng.* **1969**, *47*, T351 – T359.
[14] H. Guan, G. Guiochon, E. Davis, K. Gulakowski, D. W. Smith, *J. Chromatogr. A* **1997**, *773*, 33 – 51.
[15] U. Tallarek, K. Albert, E. Bayer, G. Guiochon, *Am. Inst. Chem. Eng. J.* **1996**, *42*, 3041 – 3054.
[16] M. Hallmann, K. K. Unger, M. Appel, G. Fleischer, J. Kärger, *J. Phys. Chem.* **1996**, *100*, 7729 – 7734.

## C-Terminal Peptide Amidation Catalyzed by Orange Flavedo Peptide Amidase**

Václav Čeřovský* and Maria-Regina Kula*

The presence of a C-terminal $\alpha$-amido group on the peptide chain is essential for the biological activity of many peptide hormones.[1] Amidated peptides are usually prepared by solid-phase synthesis on benzhydrylamine resins or by the ammonolysis of C-terminal peptide esters, which can be prepared by conventional peptide synthesis. Recombinant DNA technology allows the production of longer peptides by fermentation, but these products lack the C-terminal amido group. The combination of rDNA technology with chemical modification of the C-terminus requires the laborious protection of the functional groups in the side chains. Therefore, an enzymatic method for the introduction of an $\alpha$-amido group is highly desirable.

Enzymatic amidation of peptides with ammonia as nucleophile has rarely been described.[2] Short model peptides and amino acid derivatives were amidated by protease-catalyzed ammonolysis of the corresponding esters.[3, 4] In spite of the advantages of enzymatic methods in peptide synthesis,[5] the application of proteases for peptide amidation is limited, mainly by the risk of undesired proteolysis. In 1990 we isolated an unusual enzyme which can hydrolyze peptide amides at the C terminus without cleavage of peptide bonds or amido groups in the side chain.[6] The enzyme was isolated from the flavedo of oranges and characterized as a peptide amidase.[7] The broad substrate specificity of the enzyme makes it universally applicable for the deprotection of $\alpha$-carboxy groups in enzymatic peptide synthesis.[5]

Our aim was to use the peptide amidase to catalyze the reverse reaction, that is, the C-terminal amidation of peptides [Eq. (1); $R^1$ = amino acid residue or peptide residue; $R^2$ = side chain of an amino acid), which has not been described

$$R^1CONHCH(R^2)COOH + NH_3 \overset{\text{amidase}}{\rightleftharpoons} R^1CONHCH(R^2)CONH_2 + H_2O \quad (1)$$

up to now. In protease-catalyzed peptide synthesis,[5] the "kinetic approach" is generally considered more effective than the reverse of peptide hydrolysis ("thermodynamic approach").[5] Owing to the lack of esterase activity of the peptide amidase, only a thermodynamic approach was possible. In aqueous solutions the equilibrium of the amidase-catalyzed reaction lies far to the side of the hydrolysis products. Initial attempts to detect the reverse reaction with an excess of ammonium acetate in water-miscible solvents were unsuccessful.

Here we report on a more systematic study of amidation reactions with the dipeptide Z-Gly-Phe-OH (Z = benzyloxycarbonyl) as the acyl component and ammonium hydrogencarbonate as the ammonium source. When the reaction was carried out in acetonitrile in the presence of small amounts of water,[8] the peptide amide could be detected. The optimal dipeptide concentration was 0.05 M. Increasing the concentration to 0.1 M resulted in a viscous reaction mixture owing to the precipitation of the ammonium salt of the dipeptide, which excludes the substrate from the reaction. As shown in Figure 1, the optimal ratio of acyl component to ammonium hydrogencarbonate was 1:1.4. The slight excess of the ammonium salt maintains slightly alkaline conditions for

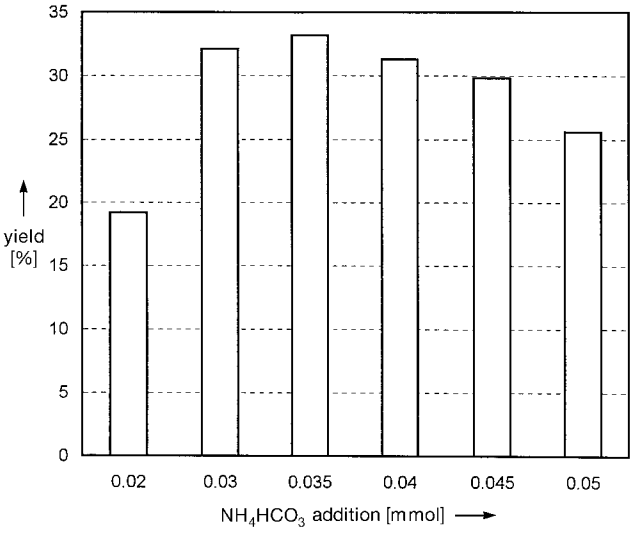


Figure 1. Influence of the ammonium concentration on the product yield in the peptide amidase catalyzed synthesis of Z-Gly-Phe-$NH_2$ in acetonitrile in the presence of 5% water. Conditions: 0.025 mmol of Z-Gly-Phe-OH, 2 mg of amidase, 0.5 mL total volume, 48 h, 40 °C.

[*] Dr. V. Čeřovský
Institute of Organic Chemistry and Biochemistry
Czech Academy of Sciences
Flemingovo 2, 166 10 Prague 6 (Czech Republic)
Fax: (+420) 2-24310090
E-mail: cerovsky@uochb.cas.cz
Prof. Dr. M.-R. Kula
Institut für Enzymtechnologie der Universität Düsseldorf
Forschungszentrum Jülich, D-52428 Jülich (Germany)
Fax: (+49) 2461-612490
E-mail: m.-r.kula@fz-juelich.de

[**] This work was supported by a fellowship of the Alexander von Humboldt Stiftung to V.Č. and by the Grant Agency of the Czech Republic (grant 203/95/0014).

  1433-7851/98/3713-1885 $ 17.50+.50/0 